



OPEN

A serotonin-induced N-glycan switch regulates platelet aggregation

SUBJECT AREAS:

SECRETION
HYDROLASES
BIOCHEMISTRY
GLYCOBIOLOGYCharles P. Mercado¹, Maritza V. Quintero³, Yicong Li¹, Preeti Singh¹, Alicia K. Byrd¹, Krajang Talabnin², Mayumi Ishihara², Parastoo Azadi², Nancy J. Rusch¹, Balagurunathan Kuberan³, Luc Maroteaux⁴ & Fusun Kilic¹

¹Departments of Biochemistry and Molecular Biology, and Pharmacology and Toxicology, College of Medicine, University of Arkansas for Medical Sciences, Little Rock, Arkansas, USA, ²Complex Carbohydrate Research Center, Athens, Georgia, USA, ³Departments of Medicinal Chemistry and Bioengineering, University of Utah, Salt Lake City, Utah, USA, ⁴INSERM UMR S-839, Institut du Fer a Moulin, 17 rue du Fer a Moulin, 75005 Paris, France.

Received
28 May 2013Accepted
30 August 2013Published
30 September 2013Correspondence and
requests for materials
should be addressed to
F.K. (kilicfusun@uams.
edu)

Serotonin (5-HT) is a multifunctional signaling molecule that plays different roles in a concentration-dependent manner. We demonstrated that elevated levels of plasma 5-HT accelerate platelet aggregation resulting in a hypercoagulable state in which the platelet surface becomes occupied by several glycoproteins. Here we study the novel hypothesis that an elevated level of plasma 5-HT results in modification of the content of N-glycans on the platelet surface and this abnormality is associated with platelet aggregation. Mass spectrometry of total surface glycoproteins on platelets isolated from wild-type mice infused for 24 hours with saline or 5-HT revealed that the content of glycoproteins on platelets from 5-HT-infused mice switched from predominantly N-acetylneuraminic acid (Neu5Ac) to N-glycolylneuraminic acid (Neu5Gc). Cytidine monophosphate-N-acetylneuraminase hydroxylase (CMAH) synthesizes Neu5Gc from Neu5Ac. Up-regulation of Neu5Gc content on the platelet surface resulted from an increase in the catalytic function, not expression, of CMAH in platelets of 5-HT-infused mice. The highest level of Neu5Gc was observed in platelets of 5-HT-infused, 5-HT transporter-knock out mice, suggesting that the surface delineated 5-HT receptor on platelets may promote CMAH catalytic activity. These new findings link elevated levels of plasma 5-HT to altered platelet N-glycan content, a previously unrecognized abnormality that may favor platelet aggregation.

Serotonin or 5-hydroxytryptamine (5-HT) is synthesized by the intestinal enterochromaffin cells and secreted into blood¹. Although the concentration of 5-HT in plasma ([5-HT]pl) is tightly regulated by the 5-HT transporter (SERT) expressed on the platelet surface², elevations of [5-HT]pl have been reported in a variety of cardiovascular pathologies including hypertension, atherosclerosis, coronary artery disease, angina and arterial thrombosis^{3–12}. Since these conditions share platelet activation as a disease component, attention has focused on identifying the complex mechanisms by which 5-HT may promote platelet activation^{13–25}.

A role in platelet aggregation for the 5-HT receptor, 5-HT_{2A}, expressed on the platelet plasma membrane (PM) is well recognized^{13–19}. Activation of the 5-HT_{2A} receptor initiates G-protein-dependent signaling in platelets, which elevates intracellular calcium to trigger the release of procoagulant molecules including 5-HT from α -granules. Tissue transglutaminase and factor XIIIa can utilize the circulating 5-HT molecules to serotonylate procoagulant proteins, which bind to the platelet surface to establish a subpopulation of highly procoagulant collagen and thrombin-activated (COAT) platelets^{23,24}. Additionally, serotonylation of cytoplasmic small GTPases promotes α -granule release^{20,21}. Thus, block of 5-HT uptake by selective 5-HT reuptake inhibitors (SSRI) attenuates platelet activation and increases bleeding time^{21,22,25}. Additionally, platelets from TPH1 knock out (KO) mice lacking the tryptophan hydroxylase 1 (TPH1) gene that encodes the rate-limiting enzyme in peripheral 5-HT synthesis show blunted α -granule secretion, and accordingly the 5-HT –depleted TPH1 KO mice show a reduced risk of thrombosis compared to wild type (WT) mice²¹. Still, the mechanisms by which 5-HT and other procoagulant molecules modify the platelet surface to make it more adhesive remain elusive.

We reported earlier that WT mice infused with 5-HT for 24 hr to elevate [5-HT]pl showed increased bleeding times and their platelets exhibited accentuated collagen induced aggregation²². Accentuated aggregation also was observed in isolated platelets from untreated WT mice exposed to extracellular 5-HT *in vitro*²². Both *in vivo* and *in vitro*, elevated 5-HT increased the surface expression of the markers of murine platelet activation, such as integrin



α IIb β 3, von Willebrand factor (vWF) and P-selectin²². Ultimately, the activation of platelets was associated with the appearance of several *N*-glycans on the platelet surface.

Platelets, anucleated megakaryocyte (MK) subfragments, contain an organized glycosylation apparatus. Golgi elements containing glycosyltransferases required for glycosylation reactions are packaged into vesicles and transported from the MK to the nascent platelets, where they distribute intracellularly as well as to the PM. It was shown that activation of platelets releases substantial glycosyltransferase activity indicating the presence of a sufficient pool of sugar nucleotides to support *in vitro* glycosylation reactions^{26,27}. The factors involved in the activation of platelet glycosyltransferases are not known. However, it is recognized that the sialic acids, which occupy the terminal positions of *N*-glycans, play important roles as ligands for receptors including the P- and E-selectins that regulate a number of cell-cell adhesive events in vascular pathophysiological processes²⁸. There are about 40 different sialic acids but the most common one is Neu5Ac which is a substrate for CMP-N-acetyl-neuraminic acid hydroxylase (CMAH) to synthesize Neu5Gc. CMAH is widely distributed in mammalian tissues²⁹. Neu5Gc is found in most mammals, but humans cannot synthesize Neu5Gc because the human CMAH gene is irreversibly mutated, although Neu5Gc has been detected in human cancers and fetal samples, suggesting that mechanisms for its formation are active under some conditions^{30,31}.

Considering that elevated [5-HT]pl is associated with platelet activation and appears to promote the expression of *N*-glycans on the platelet surface, the goal of the present study was to define precise differences in surface glycan content between the platelets of saline (SAL)- and 5-HT-infused mice, and explore the mechanisms by which 5-HT achieves an altered *N*-glycan content. Nanospray-ionization mass spectrometry (NSI-FTMS) analysis of total glycoproteins on the platelet PM of SAL-infused mice demonstrated a relative dominance of N-acetyl-neuraminic acid (Neu5Ac), but platelet PM from 5-HT-infused WT mice showed a predominance of N-glycolyl-neuraminic acid (Neu5Gc) containing *N*-glycans. These findings concurred with FACS analysis of platelets stained with Neu5Gc antibodies (Ab). Microarray analysis of genes isolated from megakaryocytes in bone marrow of SAL- and 5-HT-infused mice identified CMAH as one of the genes expressed in megakaryocytes³². Furthermore, the catalytic activity but not the expression level of CMAH was increased 3-fold in platelets of 5-HT-infused compared to SAL-infused mice. Finally, the catalytic function of CMAH was tested using 5-HT infused WT mice and two KO mouse models. The highest CMAH catalytic activity and Neu5Gc levels were identified in platelet lysates of 5-HT infused SERT KO mice, implicating 5-HT_{2A} receptor signaling as a positive regulator of CMAH activity. In contrast, TPH1 KO mice with depleted plasma 5-HT levels exhibited low Neu5Gc content. Thus, we propose a novel mechanism by which rises in [5-HT]pl signal through 5-HT_{2A} to modify the *N*-glycan composition on the platelet PM to promote aggregation.

Results

The surface of hyperreactive platelets is furnished with several glycoproteins. When plasma 5-HT level was elevated for 24 hours in mice, their platelets became hyperreactive, the rate of aggregation was increased and bleeding time was shortened²². The surface expression of the staining of markers of murine platelet activation, such P-selectin, granulophysin, vWF and P^βJon/A were increased following administration of 5-HT (Table 1). Therefore, here we investigated if elevated plasma 5-HT ([5-HT]pl) is associated with an altered density and/or composition of *N*-glycans on the platelet surface as a novel mechanism to promote platelet aggregation.

This hypothesis was investigated using platelets from C57BL/6J mice (WT) and TPH1 KO²¹ and SERT KO mice³³. The KO mice were backcrossed into the C57BL/6J background to achieve genetic

Table 1 | Analysis by flow cytometry of marker proteins associated with platelet activation

Antibody	Mean Fluorescence	
	SAL-infused	5-HT-infused
Integrin α IIb β III	36.92 \pm 2.41	115.32 \pm 12.27
P-selectin	181.7 \pm 8.00	316.05 \pm 2.61
Granulophysin	50.3 \pm 0.97	104 \pm 14.66
vWF	821.68 \pm 48.9	1088.69 \pm 123.8

homogeneity. Osmotic mini-pumps filled with saline or 5-HT were implanted subcutaneously into mice for 24 hr; then platelets were isolated and characterized for biochemical and physiological properties (Table 2). As expected, the 5-HT uptake rate of platelets isolated from SERT KO mice was below detection threshold. Similarly, plasma 5-HT concentration in TPH1 KO mice also was below detection level (Table 2).

We explored differences in the aggregation responses between platelets isolated from WT mice after 24 hours of infusion with saline (SAL) or 5-HT. Platelets were stimulated with ADP or collagen, which promote platelet aggregation by different mechanisms. Collagen-induced platelet aggregation relies on a release of 5-HT from platelets and is accepted as a primary hemostatic agonist, whereas ADP (released from platelet dense granules) is a secondary stimulant. Platelets isolated from 5-HT- and SAL-infused mice were prepared and stimulated with increasing concentrations of ADP (5, 10 and 20 μ M) to test the effect of elevated 5-HT on their stirred platelet aggregation assays (Figure 1A). The aggregation response of the platelets to ADP was enhanced in platelets from 5-HT -infused mice. For example, the average peak aggregation response to 20 μ M ADP in a triplicate platelet preparations was 50 \pm 7% (SAL) and 65 \pm 5% (5-HT). A more pronounced effect of elevated [5-HT]pl was observed for collagen-stimulated platelets. Representative tracings reveal an enhanced collagen (4 μ g/ml) -induced aggregation response of platelets from 5-HT compared to SAL-infused mice (Figure 1B), which averaged 35 \pm 8% and 70 \pm 8% after ten minutes, respectively (Figure 1C).

The identity of the 5-HT signaling mechanism involved in promoting platelet aggregation was examined by injecting mice with the 5-HT_{2A} receptor antagonist, sarpogrelate (Sarp, 30 mg/kg i.p.) 18 hours after implanting SAL- or 5-HT-containing minipumps^{35,36}. Six hours later, blood was drawn and platelets were isolated to evaluate the effect of Sarp on platelet aggregation. Stirred platelet aggregation assays revealed that Sarp treatment did not significantly affect the aggregation response of platelets from SAL mice (not shown), but it reversed the accentuated collagen-induced aggregation of platelets from 5-HT-infused mice (Figures 1B–C). Accordingly, platelets isolated from SAL and 5-HT infused mice injected with Sarp showed a 35% and ~43% reduction, respectively, in the surface expression of the P-selectin platelet activation marker compared to platelets from untreated mice (Figure 1D). After Sarp treatment, the elevated P-selectin expression in platelets of 5-HT mice was restored to a level not significantly different than untreated SAL mice. These findings suggest that elevated [5-HT]pl initiates intraplatelet 5-HT_{2A} receptor signaling associated with enhanced aggregation and activation.

Next we investigated the total *N*-glycan content on plasma membranes (PM) isolated from an equal number of platelets from the blood samples of SAL- and 5-HT-infused mice³⁷. *N*-glycans were enzymatically released from glycoproteins on the platelet PM by PNGase F and PNGase A treatment. After purification, released *N*-glycans were subjected to per-*O*-methylation prior to NSI-FTMS analysis (Figures 2A–B)^{38,39}. The total released sialylated *N*-glycans were not significantly different between platelet PM of SAL- and 5-HT-infused mice (Figure 2C). However, the relative abundance of



Table 2 | Summary of findings in 6 groups of mice

	WT	WT + 5-HT	SERT-KO	SERT-KO + 5-HT	TPH1-KO	TPH1-KO + 5-HT
[5-HT] in plasma (ng/μl blood)	0.85 \pm 0.04	2.74 \pm 0.37	1.75 \pm 0.05	3.54 \pm 0.16	u.n.d.	2.14 \pm 0.4
[5-HT] in platelet (ng/μl blood)	5.15 \pm 0.89	5.77 \pm 0.54	u.n.d.	u.n.d.	u.n.d.	4.97 \pm 0.5
5-HT uptake rates (pmol/min/mg protein)	0.76 \pm 0.08	0.48 \pm 0.05	u.n.d.	u.n.d.	0.89 \pm 0.04	0.45 \pm 0.08
Percent aggregation rate	35.8 \pm 8.06	70.7 \pm 7.63	25.67 \pm 5.03	34.67 \pm 4.16	31.67 \pm 5.77	60 \pm 3.54
Flow Cytometry analysis of P-selectin	181.7 \pm 8.00	316.05 \pm 2.61	96.15 \pm 9.76	105.46 \pm 11.8	93.13 \pm 7.77	195.38 \pm 13.11
Ratio Neu5Gc/Neu5Ac (LC-MS results)	0.61 \pm 0.04	1.73 \pm 0.3	0.68 \pm 0.03	3.88 \pm 0.32	0.43 \pm 0.07	2.13 \pm 0.24

u.n.d. = undetectable; defined as [5-HT] < 0.1 ng/ml or 5-HT uptake rate less than the background accumulation of 3 H-5HT.

Neu5Ac in total N-glycans released from the platelet PM of 5-HT mice was 61.6% lower compared to SAL-infused mice. Reciprocally, the relative abundance of Neu5Gc was 70.3% higher in platelet PM of 5-HT mice compared to SAL mice (Figures 3A–B). The Neu5Ac/Neu5Gc ratio on the PM of platelets obtained from SAL mice was 2.89, whereas the reciprocal Neu5Gc/Neu5Ac ratio on platelets from 5-HT mice was 3.03 (Figures 3A–C).

Flow cytometry using platelets stained with Neu5Gc Ab concurred with the NSI-FTMS findings and showed a 33% elevation in the relative abundance of Neu5Gc in platelets isolated from 5-HT mice compared to SAL mice (Figures 4A–B). Thus, exposure to elevated [5-HT]pl for 24 hours *in vivo* conferred heightened Neu5Gc levels

associated with increased activation of the affected platelets as evidenced by enhanced collagen-induced aggregation and P-selectin surface expression (Figure 1B–C; Tables 1 and 2). Since the increase in Neu5Gc-containing N-Glycans on the PM of platelets from 5-HT mice suggested enhanced CMAH-mediated conversion of Neu5Ac to Neu5Gc, we explored whether elevated [5-HT]pl alters the expression or catalytic activity of CMAH in platelets.

Microarray analysis detected CMAH in MK (not shown), so we chose to examine the expression level of the CMAH transcript in platelets using specific primers (Table 3) and RT-PCR analysis. Parallel amplification reactions evaluated the relative abundance of the CMAH transcript in other blood cell components (red blood cell,

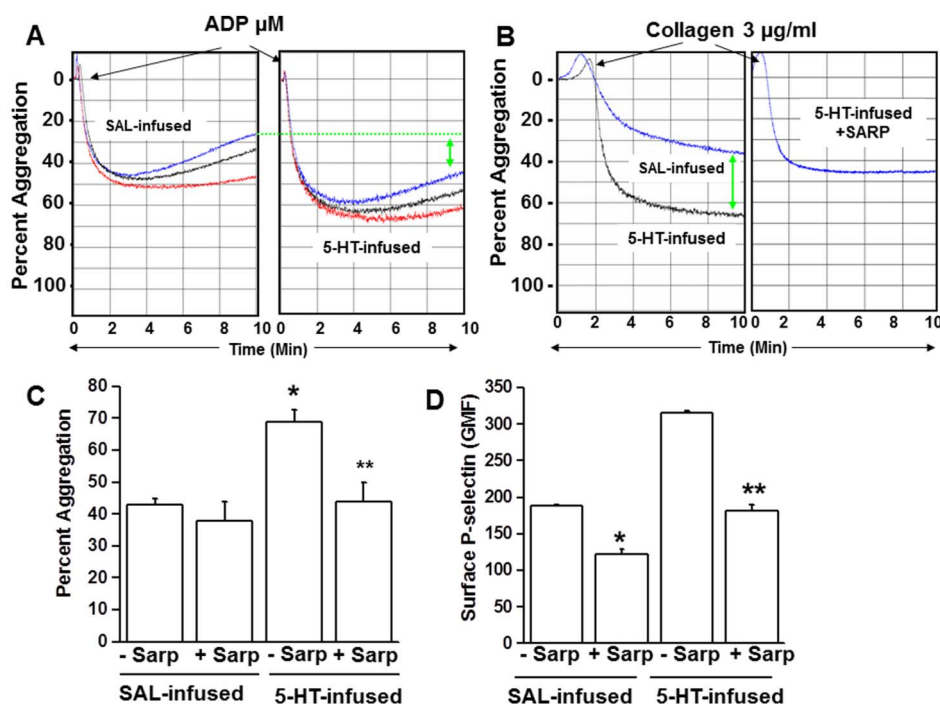


Figure 1 | (A) Aggregation of isolated platelets following 5-HT infusion. Comparison of light-transmission aggregation profiles in platelets isolated from saline- vs. 5HT-infused C57BL/6J mice (WT) in response to ADP (5, 10, 20 μ M, shown in red, black and blue lines on the graph, respectively). Platelets exposed to elevated plasma 5-HT showed accentuated aggregation. (B) Collagen-induced aggregation and effect of sarpegrelate (Sarp). Platelets isolated from 5-HT infused mice showed an enhanced aggregation response to collagen (4 μ g/mL) compared to platelets from saline (SAL) –infused mice. The 5-HT_{2A} receptor antagonist, Sarp (30 mg/g of body weight), was injected after 18 hr of 5-HT infusion and animals were sacrificed at 24 hr. Platelets isolated from Sarp-injected 5-HT-mice showed normal aggregation profiles. (C) Percent aggregation. Approximately 45% of the platelets from Sarp-injected saline-infused mice and 55% of platelets from Sarp-injected 5-HT-infused mice were aggregated at the end of 10 min, whereas in the absence of Sarp, platelets from saline- and 5-HT mice showed ~35% and ~65% aggregation, respectively. (D) Effect of Sarp on surface P-selectin expression. The effect of Sarp-injection on the plasma membrane level of p-Selectin was measured by FACS analysis and calculated as the geometric mean of fluorescence (GMF). Expression of p-Selectin was much lower in Sarp-injected mice even after 5-HT infusion. An average of 5 measurements are presented in bar graphs. Asterisks indicate statistical difference between saline- and Sarp-injected saline-infused (*) and 5-HT- and Sarp-injected 5-HT-infused (**) mice. All assays were performed in triplicate (n = 15/group).

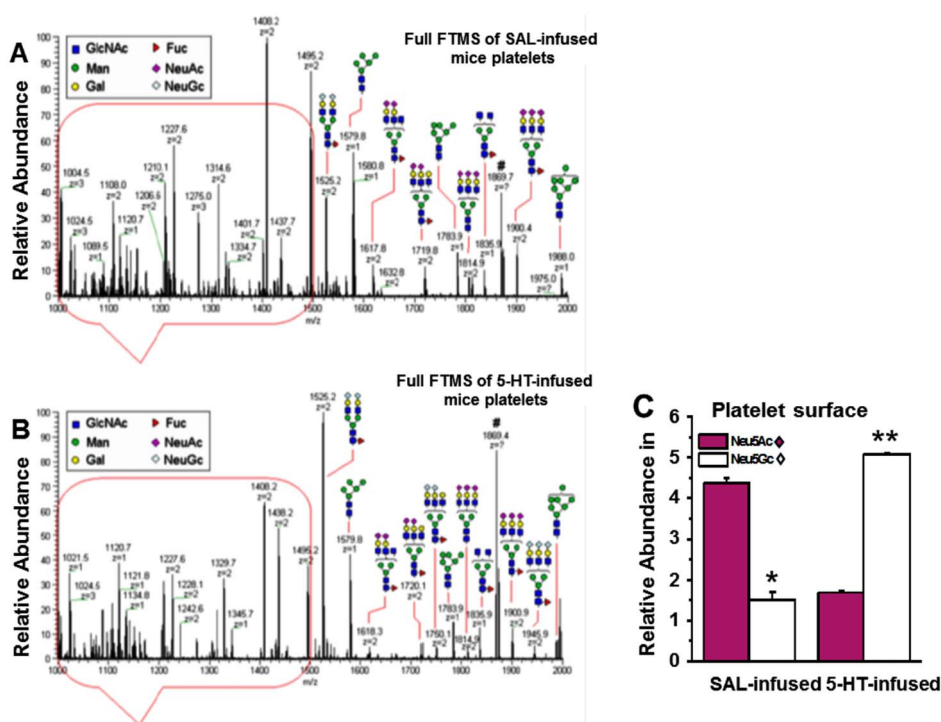


Figure 2 | NSI-MS spectra of permethylated *N*-glycans from platelets of saline (SAL) (A) and 5-HT-infused (B) mice. An equal number of platelets from WT mice infused for 24 hr with SAL or 5-HT were collected and plasma membrane (PM) was isolated³⁴. The *N*-linked glycans on membrane vesicles were released enzymatically by PNGase F. Released *N*-glycans were permethylated and profiled by an LTQ Orbitrap Discoverer mass spectrometer equipped with a nanospray ion source. Glycans are detected as singly $[M + Na]^+$, doubly $[M + Na]^{2+}$ and triply $[M + Na]^{3+}$ charged species. Structural assignments are based on MS/MS fragmentation and known biosynthetic limitation^{38,39}. (C) The relative abundance of Neu5Ac on the platelet PM of SAL-infused mice was 2.9-fold higher than Neu5Gc containing glycans, whereas the ratio for platelet PM of 5-HT-infused mice was 3-fold higher in Neu5Gc-containing glycans than Neu5Ac. The total Neu5Ac and Neu5Gc-containing glycans was not different between platelet PM of SAL and 5-HT mice.

RBC; buffy coat, BC primarily containing white blood cells) to determine if CMAH is preferentially expressed in platelets. This analysis revealed that the mRNA expression level of CMAH was significantly higher in platelets than in other blood components (Figures 5A–B). Subsequently, Western blot (WB) analysis of platelets using CMAH-Ab confirmed the presence of CMAH protein in mouse platelet lysates and further indicated that CMAH protein expression did not differ significantly between platelets from SAL and 5-HT infused mice (Figure 5C). Thus, our collective data suggest that in platelets of 5-HT-infused mice: (i) Neu5Gc content in the PM is elevated whereas the level of Neu5Ac is reduced (Figures 2, 3, 4); and (ii) CMAH is expressed as a native platelet protein (Figure 5C), but its expression is not modulated by elevations of $[5-HT]_{pl}$.

Next, we evaluated the impact of 5-HT on CMAH hydroxylase activity in platelet lysates^{40–42} as the source of CMAH. Platelet lysate was reacted with CMP-Neu5Ac (substrate) and the reaction mixture was analyzed by liquid chromatography-mass spectrometry (LC-MS) (Figures 6A–B)^{43,44}. Equal protein (60 μ g) from the BC or RBC fraction prepared from blood samples of SAL or 5-HT-infused mice were reacted with CMP-Neu5Ac⁴² and analyzed by LC-MS. Due to the unavailability of an isotopically labeled Neu5Gc standard, the relative ratio of Neu5Gc to Neu5Ac within individual samples was calculated for each group. The highest ratio was seen in platelet lysates and this ratio increased significantly in 5-HT pretreated platelets (Figure 6C). The formation of Neu5Gc appeared to be time- and CMP-Neu5Ac concentration-dependent, suggesting the formation of Neu5Gc following an enzymatic, rather than a chemical reaction (Figure 6D).

To further establish a relationship between enhanced aggregability of platelets from 5-HT mice and increased Neu5Gc formation on the platelet surface, we utilized CMAH assays to analyze platelets from SERT KO and TPH1 KO mice. CMAH efficiency was assessed by the

level of Neu5Gc relative to Neu5Ac in the platelet lysates⁴². Interestingly, the ratio of Neu5Gc to Neu5Ac in platelet lysates did not differ between SAL -infused WT and SERT KO mice. However, the ratio of Neu5Gc to Neu5Ac decreased by 30% in platelets of TPH1 KO mice compared to WT (Figure 7). Additionally, Neu5Gc and P-selectin levels on the platelet PM and the rate of platelet aggregation indicate that the Neu5Gc level on the platelet surface is correlated to the plasma 5-HT level and the aggregation rates of platelets. Collectively these findings emphasize the importance of 5-HT location on its ability to promote the catalytic ability of CMAH and suggest that it can exert a strong effect from blood plasma and does not require access to the platelet interior.

Finally, the impact of elevated $[5-HT]_{pl}$ on CMAH activity was evaluated using platelets from SERT KO and TPH1 KO mice. Platelets isolated from 5-HT-infused SERT KO mice had a 44.5% higher ratio of Neu5Gc/Neu5Ac than platelets from 5-HT-infused WT mice (Figure 7). Thus, the 5-HT signaling that promotes upward shifts of the Neu5Gc/Neu5Ac ratio relies on elevated extracellular 5-HT rather than intracellular 5-HT in platelets, since SERT KO mice are deficient in platelet 5-HT³³. The Neu5Gc/Neu5Ac ratio was 13% higher in 5-HT -infused TPH1 KO compared to WT mice, because their plasma 5-HT concentration was much less than SERT KO mice (Figure 7). Elevated plasma 5-HT in WT mice increased the relative ratio of Neu5Gc/Neu5Ac by 2.8-fold; in SERT KO and TPH1 KO mice, 5-HT infusion resulted in a 5.7- and 5.0- fold increase in plasma 5-HT concentration, respectively. These results considered in parallel with our finding that the elevated aggregability in platelets from 5-HT mice is reversed by the 5-HT_{2A} receptor blocker Sarp (Figure 1B–C), clearly indicate that elevated levels of $[5-HT]_{pl}$ alter the composition of surface glycans and that this abnormality is associated with increased platelet aggregation.

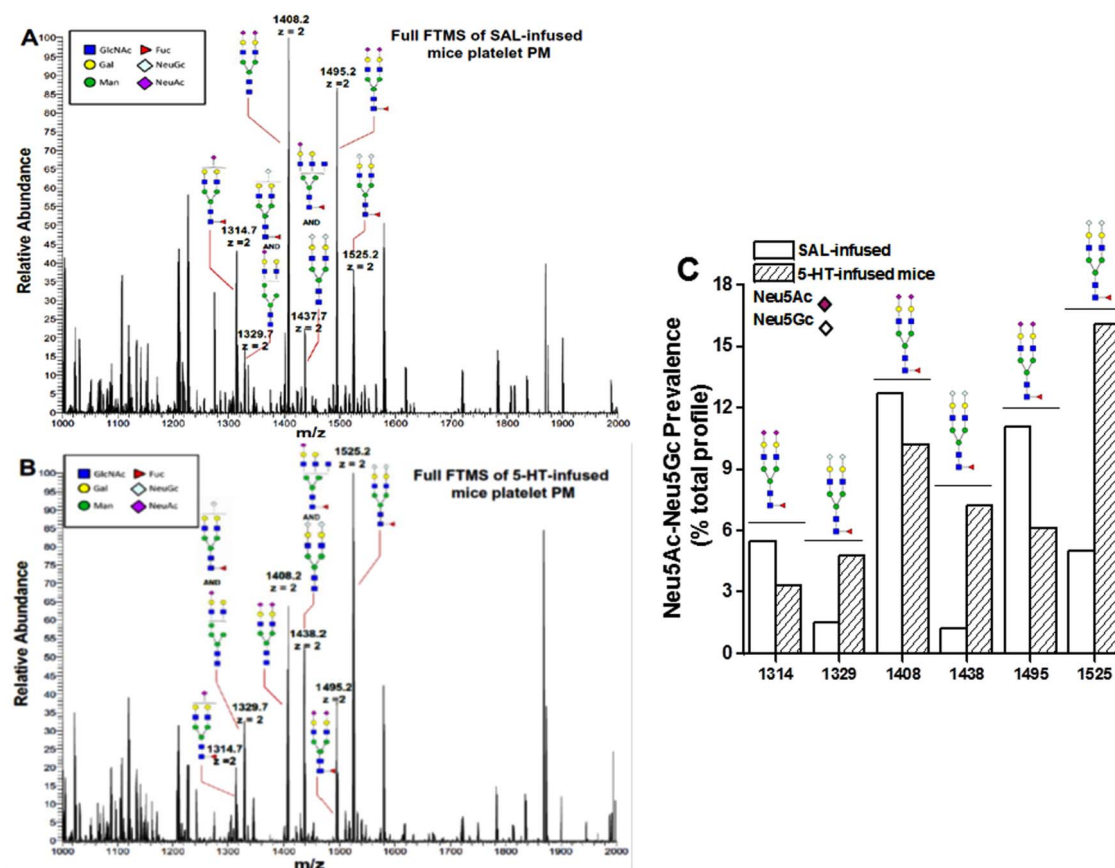


Figure 3 | NSI-MS spectra of Neu5Ac and Neu5Gc containing structures in pair. The membrane vesicles prepared from platelets of SAL- (A) or 5-HT-infused (B) WT mice show the Neu5Ac and Neu5Gc containing structures in pairs; such that 1314 ends with Neu5Ac which has a higher peak in platelets of SAL mice compared to 5-HT-infused mice. The pair for 1314 is 1329 as shown in MS/MS fragmentation, which has a lower peak in platelets from SAL- vs 5-HT-infused mice. Similarly, the pair for 1408 appears as 1438 and the pair for 1495 is 1525. (C) The ratio of Neu5Ac/Neu5Gc prevalence (% total profile) for each reaction was plotted. The bar graph presents the changes in Neu5Ac vs. Neu5Gc pairs in PM vesicles of platelets isolated from SAL and 5-HT-infused mice.

Discussion

Platelets are derived from the fragmented cytoplasm of megakaryocytes and enter the circulation in an inactive form. The initial activation of platelets stabilizes them in hemostasis. Further platelet activation enlists more platelets at a fibrin-stabilized hemostatic area to form a thrombus after associating with the endothelium or each other. The role of circulating free 5-HT in platelet adhesion, aggregation and thrombus

formation has not been resolved, but clinical and biochemical observations infer a complex involvement. For example, in carcinoid syndrome, carcinoid tumors overproduce 5-HT and the increased circulating plasma level of 5-HT (and other hormones) is correlated with the formation of disseminated intravascular coagulation¹¹. Other pathologies of increased thrombus incidence including hypertension exhibit elevated plasma 5-HT^{8–10,14,15}, and

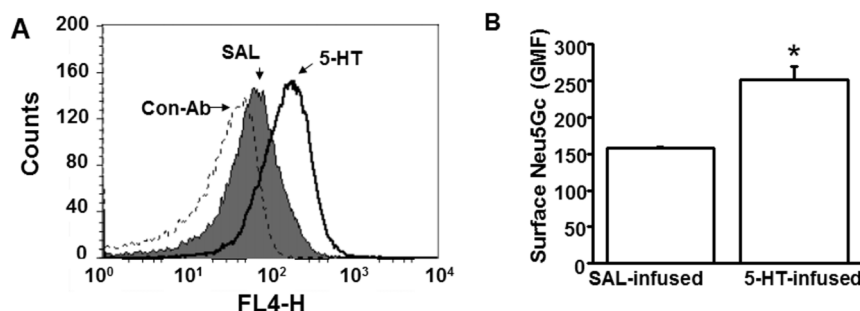


Figure 4 | Plasma membrane Neu5Gc detected by flow cytometry. (A) The impact of plasma 5-HT on the abundance of Neu5Gc containing glycans on the platelet surface was evaluated by measuring the binding of Neu5Gc to a specific Ab. Platelets (50,000/ μ l) from saline (SAL) and 5-HT-infused WT mice were stained with chicken anti-Neu5Gc IgY and anti-chicken IgY DyLight 650 as primary and secondary Ab, respectively; chicken IgY was used as a control Ab. Mean fluorescence intensity of Neu5Gc expression in platelets isolated from 5-HT-infused mice (black solid histogram) was higher than in platelets from SAL-infused mice (grey shaded area), black dashed histogram represents control IgY. (B) Geometric Mean of Fluorescence (GMF). Flow cytometry revealed an elevation of 33.5% in the expression levels of Neu5Gc in platelets of 5-HT-infused mice. * = statistical difference between SAL and 5-HT-infused mice.



Table 3 | Primer sequences for quantitative real-time PCR (qRT-PCR)

Gene	Forward Primer (5' → 3')	Reverse Primer (3' → 5')	Amplicon Size (bp)
<i>Hsp90a1b</i>	AGGCACTGCGAGACAACCTCTACAA	AGTTTCAAACAGCAGCACCACCAG	158
18s	GGGCAGCTTCCAAGAAACCAAAGT	AATTAAGCCACAGGCTCCACTCCT	114
CMAH	TTTCTAGAGAAACAGACAGCTGAGACCC	TTTGAGCTCCCGTCTAAATCCTCAATGTC	194

enhanced aggregation responses are a feature of isolated human platelets exposed to 5-HT^{21,22}.

Elevated plasma 5-HT accelerates the exocytosis of dense and α -granules in platelets^{20,21} which secrete 5-HT and other procoagulant molecules into the plasma^{14–16} to play a central role in hemostasis. In a receptor-dependent pathway, 5-HT can bind to 5-HT surface membrane receptors^{18,19} initiating a G-protein signaling pathway that mobilizes calcium from intracellular stores to trigger the vesicular release of pro-coagulant molecules^{13–21}. Additionally, activated platelets use plasma 5-HT to bind procoagulant proteins on the cell surface to form a thrombus^{14,15}. Dale *et al.*^{23,24} demonstrated that activation of platelets reveals COAT platelets, which are enriched in several membrane-bound procoagulant proteins and derivatized with 5-HT by a transglutaminase-mediated process. COAT-platelets use 5-HT conjugation to augment the retention of procoagulant proteins on their cell surface²⁴. Thus, selective 5-HT reuptake inhibitors (SSRI) that elevate plasma 5-HT also increase bleeding^{21,22,25}. Additionally, a contribution of intracellular 5-HT to receptor-independent platelet aggregation pathways has been demonstrated. 5-HT in the platelet cytosol is transamidated on small GTPases converting them to their active, GTP-bound form to enhance Ca²⁺-induced α -granule secretion^{12,20–22}. Concurrently, the association between Rab4-GTP and SERT tethers the transporter to an intracellular compartment to prevent further rises in cytoplasmic 5-HT^{22,45}.

Here, we provide initial evidence for a new mechanism by which 5-HT may contribute to platelet activation and thrombosis. Relying on platelets isolated from SAL and 5-HT-infused WT mice and from two distinct mouse models of 5-HT depletion, our data suggest that elevated plasma 5-HT may directly modify the platelet surface to establish a more adhesive environment. Elevating plasma 5-HT with osmotic mini-pumps in the absence of other cardiovascular risk factors altered platelet function. Moreover, platelets of 5-HT-infused WT but not transgenic mice (SERT KO) exhibited heightened activation and enhanced aggregation responses (Table 2). These data raise the possibility that elevated 5-HT influences platelet biochemistry to modify the adhesive characteristics of the platelet. In searching for cell adhesion factors, sialic acid at the terminal position of *N*-glycans is reported to promote cell-cell adhesion by acting as a ligand for receptors such as P- and E-selectins²⁸. Therefore, we analyzed the sialic acid profiles of *N*-glycans isolated from the platelet surface of SAL and 5-HT mice. The NSI-FTMS analysis of total glycoproteins showed elevated Neu5Gc containing *N*-glycans on platelets from 5-HT mice. Since Neu5Gc is formed from Neu5Ac via the catalytic action of CMAH, the predominance of Neu5Gc on platelets of 5-HT mice suggested enhanced CMAH activity.

The expression of CMAH in platelets has not been documented to our knowledge. Therefore, as part of a broader microarray analysis of genes in MK, we located CMAH in mouse MK and found that the

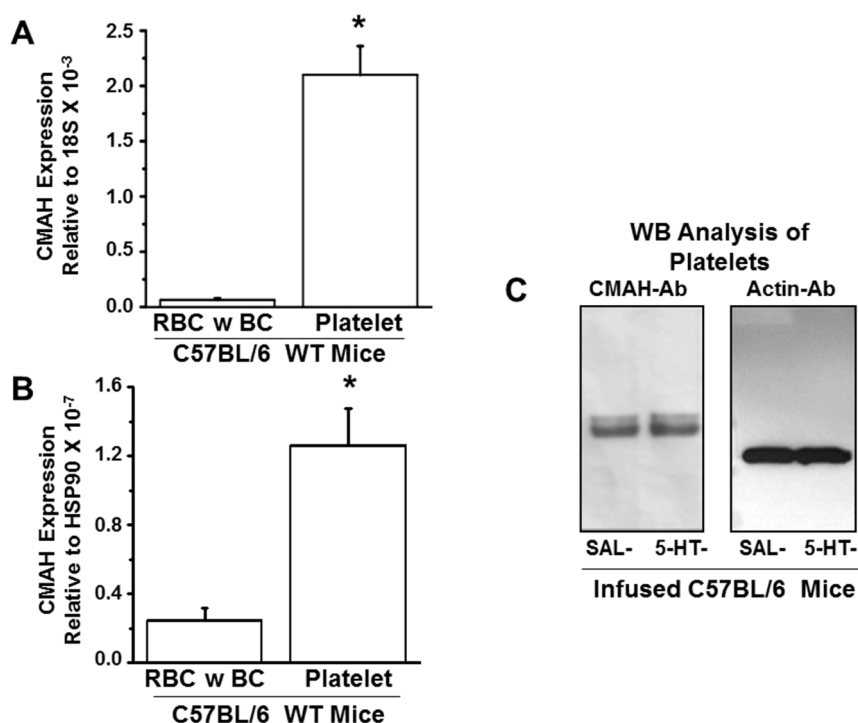


Figure 5 | Expression of CMAH genes and proteins in fractionated blood samples of WT mice. The mRNA expression levels of CMAH genes in red blood cells (RBC) and buffy coat (BC containing white blood cells) and in platelets of WT mice were normalized to the housekeeping genes 18S (A) and *Hsp90* (B). The expression level of the CMAH transcript was most abundant in platelets. Primer sequences used in qRT-PCR are listed in Table 3. (C) WB analysis of CMAH in platelets revealed that CMAH protein was similarly expressed in platelets from saline (SAL) and 5-HT-infused mice. Actin was used as a loading control. Both gels were run under the same conditions.

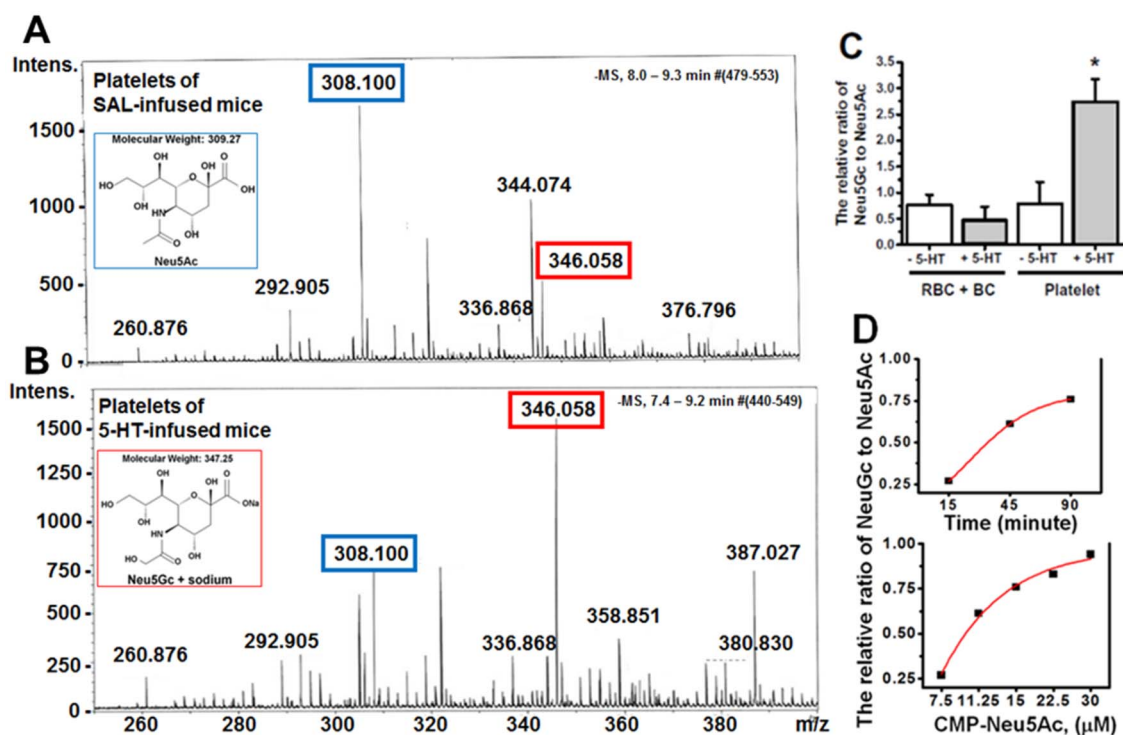


Figure 6 | LC-MS analysis of the CMAH reaction mixture. Equal numbers of platelets from saline-infused WT mice (A) and 5-HT-infused WT mice (B) were prepared for CMAH enzymatic assay. Platelet lysates were resuspended in enzyme assay buffer containing TX-100 as described in the Methods. The platelet lysate in enzyme reaction buffer was mixed with 22.5 μ M substrate (CMP-Neu5Ac) and incubated at 37°C for 45 min²⁸. The reaction mixture was analyzed with LC-MS for the level of Neu5Gc formation, and the neuraminic acid monosaccharides, Neu5Ac and Neu5Gc, were resolved as described in the Methods. Platelets from mice infused with SAL showed a higher peak corresponding to Neu5Ac (blue rectangle), whereas platelets from mice infused with 5-HT predominantly showed Neu5Gc (red rectangle). (C) The LC-MS analysis of blood fractions for CMAH. Equal amounts of protein lysate (60 μ g) from the RBC + BC component, or from platelets (as the source of enzyme) were incubated with CMP-Neu5Ac (substrate) and the reaction continued 45 min before analysis by LC-MS to determine conversion of Neu5Ac to Neu5Gc⁴⁴. The highest relative ratio of Neu5Gc to Neu5Ac was formed in the reaction mixture from platelets exposed to elevated levels of plasma 5-HT. (D) Time and substrate concentration-dependence of CMAH. Neu5Gc formed in the CMAH assay described under “Methods” was monitored by LC-MS as a function of incubation time using 60 μ g of platelet protein per assay. CMP-Neu5Ac was used as a substrate at a concentration of 11.25 μ M and the reaction followed to ensure an enzymatic rather than chemical profile.

CMAH transcript was preferentially expressed in platelets compared to other blood cell types. Next, we evaluated the impact of 5-HT on the catalytic rate of CMAH using an *in vitro* assay. Platelet lysates as the enzyme source were incubated with the CMAH substrate, CMP-Neu5Ac, and formation of the Neu5Gc product was measured by LC-MS. These data revealed increased CMAH catalytic activity in platelets from 5-HT mice. Importantly, CMAH catalytic activity was not significantly different between platelet lysates from saline-infused WT, SERT KO and TPH1 KO mice. However, in similar 5-HT-infused mice, the platelet lysate from SERT KO mice (deficient in intracellular 5-HT) showed nearly 2-fold higher CMAH activity than the lysate of WT mice. This finding infers that 5-HT signaling enhances the catalytic function of CMAH via a 5-HT_{2A} receptor-dependent pathway, enabling the elevation of a Neu5Gc population on the platelet surface. Yet, we noted that the aggregation response of platelets was not elevated (Table 2), indicating the requirement of other factors in addition to glycan structure for platelet aggregation, such as a requirement of 5-HT in the platelet cytosol to accelerate the rate of membrane trafficking. This indicates that plasma 5-HT at a high level elevates the Neu5Gc level on platelet surface, not only promoting its biosynthesis through the catalytic activity of CMAH but also promoting the translocation rates of the vesicles carrying Neu5Gc containing N-glycans to the plasma membrane. At this point, the involvement of Neu5Gc in platelet adhesion is unknown, but the predominant expression of Neu5Gc on tumor cells may infer a role in cell adhesion^{29,46,47}.

Neither the impact of 5-HT on platelet glycan content nor the types of glycans which may enhance the adhesive properties of platelets have been reported or presented before the current studies. Although only correlative at this point, our novel findings provide strong evidence that the elevated plasma 5-HT is associated with an enhanced propensity for platelet aggregation, and one potential contributing mechanism may be a switch in the surface N-glycan components from Neu5Ac to Neu5Gc via a 5-HT_{2A}-dependent signaling pathway. Notably, plasma 5-HT is elevated in a number of cardiovascular pathologies and platelet 5-HT content is reportedly reduced, suggesting that these events are worthy of study as potential contributors to the clustering of cardiovascular diseases that may predispose to thrombosis. Humans cannot synthesize Neu5Gc, but Neu5Gc has been detected in neoplastic disease³⁰, and Neu5Gc-rich foods have been proposed to deliver immunogenic Neu5Gc to humans which contributes to anti-Neu5Gc antibody- and complement-dependent activation and potentially contributes to human vascular pathologies⁴⁸. Immuno-analysis of human vascular tissue has revealed an overexpression of Neu5Gc in the endothelium overlying atherosclerotic plaques and Neu5Gc was observed to accumulate within atheromas, suggesting a possible role in accelerated inflammation⁴⁸. These findings suggest the link between altered platelet N-glycan content and platelet function in humans may be an exciting avenue to explore, and our novel findings raise the possibility that modified N-glycan profiles on the platelet surface may potentially lead to altered interaction with other platelets or the blood

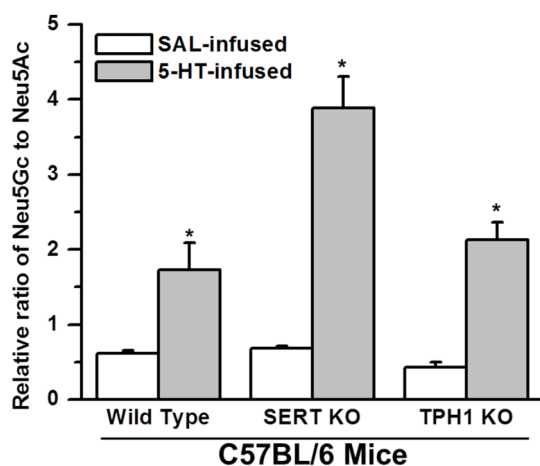


Figure 7 | Neu5Ac and Neu5Gc. Equal numbers of platelets (~60 μg protein) were separated from the blood samples of saline (SAL)–infused or 5-HT-infused WT, SERT KO, or TPH1 KO mice. Platelets were resuspended in enzyme assay buffer containing TX-100 and lysed. The platelet lysate in the enzyme reaction buffer was mixed with 12 μM substrate (CMP-Neu5Ac) and incubated at 37°C for 45 min. The reaction mixture was analyzed with LC-MS and the levels of Neu5Gc formation were measured in each group. The highest amount of Neu5Gc was formed from platelets of 5-HT-infused SERT KO mice. Asterisks indicate that 5-HT treatment elevated the catalytic ability of CMAH in the platelets of WT and KO mice significantly compared to the levels in their untreated counterparts (two-sided t-test, $p < 0.01$). Results from three independent experiments are shown (mean \pm SD).

vessel wall resulting in disruption of normal homeostatic mechanisms that regulate platelet aggregation.

Methods

Animals. Adult male C57BL/6J wild-type (WT) mice, or SERT KO and TPH1 KO mice on a C57BL6 genetic background were anesthetized with isoflurane for subcutaneous implantation of osmotic mini-pumps. Pumps were filled with saline (SAL) or 0.05 mg/ml 5-HT dissolved in saline²³ to provide an infusion rate of 1.66 $\mu\text{g}/\text{kg}/\text{hr}$. Procedures involving animals were approved by the Institutional Animal Care and Use Committee at the University of Arkansas for Medical Sciences and were conducted in accordance with the NIH Guide for the Care and Use of Laboratory Animals.

Preparation of glycopeptides and release of N-linked glycans. The platelets isolated from mouse blood samples and crude membrane vesicles were prepared as previously described³⁷. Platelet plasma membrane vesicles from the mouse models were digested with trypsin and chymotrypsin for 18 h at 37°C in 0.1 M Tris-HCl, pH 8.2, containing 1 mM CaCl_2 . The digestion products were enriched and freed of contaminants by a Sep-Pak C18 cartridge column. After enrichment, the glycopeptides were digested with 2 μl of PNGaseF (7.5 unit/ml) in 50 μl of 50 mM sodium phosphate buffer, pH 7.5, for 18 h at 37°C. Released oligosaccharides were separated from peptides and enzymes by passage through a Sep-Pak C18 cartridge column.

The glycan fraction was dissolved in dimethylsulfoxide and then permethylated as described³⁸. The reaction was quenched by addition of water and per-O-methylated carbohydrates were extracted with dichloromethane. Per-O-methylated glycans were dried under a stream of nitrogen.

Nanospray ionization-linear ion trap mass spectrometry. Mass analysis by NSI-MS was performed on a LTQ Orbitrap mass spectrometer (Thermo Scientific) equipped with a nanospray ion source. Briefly, permethylated glycans were dissolved in 1 mM NaOH in 50% methanol and infused directly into a linear ion trap mass spectrometer using a nanospray source at a syringe flow rate of 0.5 $\mu\text{l}/\text{min}$. The capillary temperature was set to 210°C, and MS analysis was performed in positive ion mode. For fragmentation by CID in MS/MS modes, 50% collision energy was applied. The nomenclature of Domon and Costello³⁹ was used to guide the depiction of fragmentation derived from MS/MS spectra.

CMAH assay. Platelet ($10^8/\text{assay}$ ~ 60 μg protein) pellet was prepared from PRP samples. Briefly, equal numbers of platelets were resuspended in 50 mM HEPES/NaOH (pH 7.4) and lysed in Triton X-100 (2.5% by mass). The platelet lysate was used as the enzyme source and mixed with substrate, CMP-Neu5Ac, at 37°C in the

presence of 1 mM NADH and 0.5 mM FeSO_4 ⁴³. The final volume of the assay was 25 μl . The assays, performed in duplicate, were stopped by the addition of 5 μl of 1 M trichloroacetic acid (TCA). The assay mixture was analyzed by LC-MS as described below⁴⁴.

Analysis of Neu5Ac and Neu5Gc using LC-ESI-TOF MS. Neuraminic acid monosaccharides, Neu5Ac and Neu5Gc, were resolved at a flow rate of 5 $\mu\text{l}/\text{min}$ on a Proto 300 C18 5 μm 250 \times 0.3 mm column (Higgins Analytical) using a linear water-acetonitrile gradient containing 5 mM dibutylammoniumacetate ion-pairing agent over 30 minutes. Mass spectra were collected using Electrospray Ionization-Time of Flight MS (Bruker Daltonics) in negative ionization mode using 7.0 eV collision energy, 3500 V capillary potential and a source temperature of 180°C^{43,44}. Nitrogen was used as drying gas (4 L/min) and nebulizer (0.4 bar). Mass spectra were analyzed using Data Analysis 2.2 software (Bruker Daltonics).

Full Methods and any associated references are available in the supplementary information.

- Barter, R. & Pearce, A. G. Mammalian enterochromaffin cells as the source of serotonin (5-hydroxytryptamine). *J Pathol Bacteriol.* **69**, 25–31 (1955).
- Rudnick, G. & Nelson, P. J. Reconstitution of 5-hydroxytryptamine transport from cholate-disrupted platelet plasma membrane vesicles. *Biochemistry.* **28**, 5300–5303 (1978).
- Vikenes, K., Farstad, M. & Nordrehaug, J. E. Serotonin is associated with coronary artery disease and cardiac events. *Circulation.* **100**, 483–489 (1999).
- van den Berg, E. K. *et al.* Transcardiac serotonin concentration is increased in selected patients with limiting angina and complex coronary lesion morphology. *Circulation.* **79**, 116–124 (1989).
- Ni, W. & Watts, S. W. 5-hydroxytryptamine in the cardiovascular system: focus on the serotonin transporter (SERT). *Clin Exp Pharmacol Physiol.* **33**, 575–583 (2006).
- Ban, Y. *et al.* Impact of increased plasma serotonin levels and carotid atherosclerosis on vascular dementia. *Atherosclerosis.* **95**, 153–159 (2007).
- Freyburger, W. A. *et al.* The pharmacology of 5-hydroxytryptamine (serotonin). *J Pharmacol Exp Ther.* **105**, 80–86 (1952).
- Vanhoutte, P. M. Platelet-derived serotonin, the endothelium, and cardiovascular disease. *J Cardiovasc. Pharmacol.* **17**(Suppl. 5), S6–12 (1991).
- Reed, G. L. Platelet Secretion. *Platelets*. Michelson, A. D. (ed), 309–319 (Academic Press, 2006).
- White, J. G. Platelet Structure *Platelets* Michelson, A. D. (ed), 45–75 (Academic Press 2006).
- Miller, F., Friedman, R., Tanenbaum, J. & Griffin, A. Disseminated intravascular coagulation and acute myoglobinuric renal failure: A consequence of the serotonergic syndrome. *J Clin Psychopharm.* **11**, 277–279 (1991).
- Roth, B. L. Drugs and valvular heart disease. *NEJM.* **356**, 6–9 (2007).
- McNicol, A. & Israel, S. J. Platelets and anti-platelet therapy. *J Pharmacol Sci.* **93**, 381–396 (2003).
- De Clerck, F. F. & Herman, A. G. 5-Hydroxytryptamine and platelet aggregation. *Fed Proc.* **42**, 228–232 (1983).
- De Clerck, F. F. & Janssen, P. A. Amplification mechanisms in platelet activation and arterial thrombosis. *J Hypertens.* **8**, S87–93 (1990).
- Nakamura, K., Kariyazono, H., Masuda, H., Sakata, R. & Yamada, K. Effects of sarpagolate hydrochloride on platelet aggregation, and its relation to the release of serotonin and P-selectin. *Blood Coagul Fibrinolysis.* **10**, 513–519 (1999).
- Berry, C. N. *et al.* Antiplatelet and antithrombotic activity of SL65.0472, a mixed 5-HT_{1B/5-HT_{2A}} receptor antagonist. *Thromb Haemost.* **85**, 521–528 (2001).
- Nishihiro, K. *et al.* Inhibition of 5-hydroxytryptamine receptor prevents occlusive thrombus formation on neointima of the rabbit femoral artery. *J Thromb Haemost.* **4**, 247–255 (2006).
- Przyklenk, K. *et al.* Targeted inhibition of the serotonin 5HT_{2A} receptor improves coronary patency in an in vivo model of recurrent thrombosis. *J Thromb Haemost.* **8**, 331–340 (2010).
- Shirakawa, R. *et al.* Small GTPase Rab4 regulates Ca^{2+} -induced α -granule secretion in platelets. *J Biol Chem.* **275**, 33844–33849 (2000).
- Walther, D. J. *et al.* Serotonylation of small GTPases is a signal transduction pathway that triggers platelet alpha-granule release. *Cell.* **115**, 851–862 (2003).
- Ziu, E. *et al.* Down-regulation of the serotonin transporter in hyperreactive platelets counteracts the pro-thrombotic effect of serotonin. *J Mol Cell Cardiol.* **5**, 1112–1121 (2012).
- Dale, G. L. *et al.* Stimulated platelets use serotonin to enhance their retention of procoagulant proteins on the cell surface. *Nature.* **4**, 175–179 (2002).
- Dale, G. L. Coated-platelets: an emerging component of the procoagulant response. *J Thromb Haemost.* **3**, 2185–2192 (2005).
- Ottervanger, J. P., Stricker, B. H., Huls, J. & Weeda, J. N. Bleeding attributed to the intake of paroxetine. *Am J Psychiatry.* **151**, 781–782 (1992).
- Hoffmeister, K. M. *et al.* Glycosylation restores survival of chilled blood platelets. *Science.* **301**, 1531–1534 (2003).
- Wandall, H. H. *et al.* The origin and function of platelet glycosyltransferases. *Blood.* **120**, 626–635 (2012).



28. Kelm, S. & Schauer, R. Sialic acids in molecular and cellular interactions. *Int Rev Cytol.* **175**, 137–240 (1997).
29. Varki, A. Glycan-based interactions involving vertebrate sialic-acid-recognizing proteins. *Nature.* **446**, 1023–1029 (2007).
30. Chou, H. H. *et al.* A mutation in human CMP-sialic acid hydroxylase occurred after the Homo-Pan divergence. *Proc Natl Acad Sci U S A.* **95**, 11751–11756 (1998).
31. Irie, A., Koyama, S., Kozutsumi, Y., Kawasaki, T. & Suzuki, A. The molecular basis for the absence of N-glycolylneuraminic acid in humans. *J Biol Chem.* **273**, 15866–15871 (1998).
32. Mercado, C. P. *et al.* Impact of elevated plasma serotonin on global gene expression of murine megakaryocytes. *PLoS One.* **8**, e72580 (2013).
33. Bengel, D. *et al.* Altered brain serotonin homeostasis and locomotor insensitivity to 3, 4-methylenedioxymethamphetamine ('Ecstasy') in serotonin transporter deficient mice. *Mol Pharmacol.* **53**, 649–655 (1998).
34. Daniel, J. L. *et al.* Molecular basis for ADP-induced platelet activation. I. Evidence for three distinct ADP receptors on human platelets. *J Biol Chem.* **273**, 2024–2029 (1998).
35. Iizuka, K., Hamaue, N., Machida, T., Hirafuji, M. & Tsuji, M. Beneficial effects of sarpogrelate hydrochloride, a 5-HT_{2A} receptor antagonist, supplemented with pioglitazone on diabetic model mice. *Endocr Res.* **34**, 18–30 (2009).
36. Bir, S. C. *et al.* New therapeutic approach for impaired arteriogenesis in diabetic mouse hindlimb ischemia. *Circ J.* **72**, 633–640 (2008).
37. Kilic, F. & Rudnick, G. Oligomerization of the serotonin transporter and its functional consequences. *Proc Natl Acad Sci USA.* **97**, 3106–3111 (2000).
38. Anumula, K. R. & Taylor, P. B. A comprehensive procedure for preparation of partially methylated alditol acetates from glycoprotein carbohydrates. *Anal Biochem.* **203**, 101–108 (1992).
39. Domon, B. & Costello, C. E. Structure elucidation of glycosphingolipids and gangliosides using high-performance tandem mass spectrometry. *Biochemistry.* **5**, 1534–1543 (1988).
40. Kozutsumi, Y. *et al.* Reconstitution of CMP-N-acetylneuraminic acid hydroxylation activity using a mouse liver cytosol fraction and soluble cytochrome b5 purified from horse erythrocytes. *J Biochem.* **110**, 429–435 (1991).
41. Shaw, L. *et al.* CMP-N-acetylneuraminic acid hydroxylase from mouse liver and pig submandibular glands. Interaction with membrane-bound and soluble cytochrome b5-dependent electron transport chains. *Eur J Biochem.* **219**, 1001–1011 (1994).
42. Chenu, S. *et al.* Reduction of CMP-N-acetylneuraminic acid hydroxylase activity in engineered Chinese hamster ovary cells using an antisense-RNA strategy. *Biochim Biophys Acta.* **1622**, 133–144 (2003).
43. Budd, T. J. *et al.* Comparison of the N-glycolylneuraminic and N-acetylneuraminic acid content of platelets and their precursors using high performance anion exchange chromatography. *Glycoconj J.* **9**, 274–278 (1992).
44. Kuberan, B. *et al.* Analysis of heparan sulfate oligosaccharides with ion pair-reverse phase capillary high performance liquid chromatography-microelectrospray ionization time-of-flight mass spectrometry. *J Am Chem Soc.* **124**, 8707–8718 (2002).
45. Ahmed, A. *et al.* Serotonin transamidates Rab4 and facilitates its binding to the C terminus of serotonin transporter. *J Biol Chem.* **283**, 9388–9398 (2008).
46. Kawano, T. *et al.* Molecular cloning of cytidine monophospho-N-acetylneuraminic acid hydroxylase. *J Biol Chem.* **270**, 16458–16463 (1995).
47. Inoue, S., Sato, C. & Kitajima, K. Extensive enrichment of N-glycolylneuraminic acid in extracellular sialoglycoproteins abundantly synthesized and secreted by human cancer cells. *Glycobiology.* **20**, 752–762 (2010).
48. Pham, T. *et al.* Evidence for a novel human-specific xeno-auto-antibody response against vascular endothelium. *Blood.* **114**, 5225–5235 (2009).

Acknowledgements

We gratefully acknowledge the UAMS Department of Animal Laboratory Medicine (DLAM) and Flow Cytometry Core, and thank Mr. Terry Fletcher for assistance in animal handling. LM is supported by the Centre National de la Recherche Scientifique, the Institut National de la Santé et de la Recherche Médicale, the Université Pierre et Marie Curie and by grants from the Foundation de France, and the French Ministry of Research (Agence Nationale pour la Recherche ANR-12-BSV1-0015-01; LM's team is part of the École des Neurosciences de Paris Ile-de-France network and of the Bio-Psy Labex).

This work was supported by the NIH National Center for Biomedical Glycomics grant to PA (8P41GM103490), NHLBI grants to KB (HL107152) and to FK [HL091196 and HL091196-01A2W1], American Heart Association [13GRNT17240014] and the Minnie Merrill Sturgis Diabetes Research Fund, and the Sturgis Charitable Trust to FK.

Author contributions

F.K. designed and directed the project; C.M., M.Q., Y.L., P.S., K.T., M.I. conducted experiments. C.M., K.T., M.I., P.A., B.K., F.K. analyzed the data. N.J.R., A.K.B., B.K., L.M., F.K. participated in manuscript writing and scientific discussions, giving detailed feedback in all areas of the project.

Additional information

Supplementary information accompanies this paper at <http://www.nature.com/scientificreports>

Competing financial interests: The authors declare no competing financial interests.

How to cite this article: Mercado, C.P. *et al.* A serotonin-induced N-glycan switch regulates platelet aggregation. *Sci. Rep.* **3**, 2795; DOI:10.1038/srep02795 (2013).



This work is licensed under a Creative Commons Attribution-NonCommercial-NoDerivs 3.0 Unported license. To view a copy of this license, visit <http://creativecommons.org/licenses/by-nc-nd/3.0>